Implication of biogeochemical change driven by global warming in the East Sea

IL NAM KIM

Department of Marine Science, University of Texas, Austin, TX 78705, USA

Abstract: The East Sea is undergoing physical changes caused by global warming: deepening oxygen minimum layer and increasing temperature. However, any correspondence to biogeochemical change was not noticed yet. Here, we present indirect evidences of denitrification in response to a global warming and estimate the amount of denitrification by the linear inverse model. N/P ratio of the East Sea below 300m is estimated as 12.4, quite lower than the Redfield ratio of 16. Intense N/P ratio and oxygen minimum zones are founded between 900m and 2200m in the Ulleung Basin. Two stations are strongly expected to occur denitrification, where is located within the Ulleung Basin, show a series of phenomena at specific depths that nitrate profile is reversed, N/P ratio is less than 12.4, and nitrite shows a peak. Evidently, these results indicate that denitrification is occurring in the East Sea, in particular, in the Ulleung Basin. Through linear inverse modeling, the mean flux of denitrification in the UB is estimated as 9.0 ~ 16.0 $\mu mol \cdot m^{-2} \cdot day$, and the mean rate is ranged from $6.38 \times 10^4 \sim 11.35 \times 10^4 mol \cdot d^{-1}$. However, note that the East Sea is still high concentration in oxygen compared with the condition denitrified. Nevertheless, considered it in relation to the recently radical changes of the East Sea, the results might be involved in biogeochemical feedback loop returning as positive effect on the climate change. Therefore, we need to note the future change of the East Sea.

Keywords: the East Sea, linear inverse model, N/P ratio and oxygen minimum, denitrification, biogeochemical feedback loop, the climate change.

1. Introduction

The East Sea is a semi-enclosed marginal sea in the North Western Pacific surrounded by Korea, Russia, and Japan. It has four straits (Korea, Tsugaru, Soya, and Tatar), three major basins (Ulleung, Yamato, and Japan), and one rise (Yamato). In the upper part of the East Sea, four straits play a role to exchange seawaters between the East Sea and the neighboring oceans, which are Okhotsk, Pacific Ocean, and the South Sea. [Fig. 1].

The East Sea is frequently cited as "Miniature Ocean", because it has a lot of oceanic characteristics- for instances, water formation, front, eddy, upwelling, and etc. In view of the time that the anthropogenic CO2 has been emitted in the atmosphere since pre-industry, the East Sea plays an optimal place as a natural model to study modern climate change [Kim et al., 2001], because the residence time of the East Sea is about 100 years [Kim and Kim, 1996; Seung and Kim, 1997; Yanagi, 2002].

Recently, many studies supported the fact that physical changes deduced from global warming are occurring in the East Sea: for examples, increases of air and sea temperature [Gamo, 1999; Min and Kim, 2006], deepening of the oxygen minimum layer [Kim and Kim, 1996; Chen et al., 1999, Kim et al., 2001; Kang et al., 2004, Kim et al., 2004], and the change of deep water formation from bottom to intermediate mode [Gamo, 1999; Gamo et al., 2001; Kang et al., 2003b, Kim et al., 2003; Chae et al., 2005]. Also, some scenarios on the possibility that

the East Sea will become an anoxic sea were represented through modeling [Chen et al., 1999; Kang et al., 2004].

It is necessary that biogeochemical change must be accompanied instantaneously with physical changes; however, any biogeochemical change in the East Sea is not noticed yet. Just, the previous literatures have been reporting that the East Sea shows quite low N/P ratio, which is ranged from 11.30 to 14.70 [Table 1]. The reason is now unclear, but recently a few scientists carefully assume the reason that denitrification is occurring in the East Sea – for examples, Yanagi [2002] suggested the possibility through nitrogen budget in terms of mass balance, and Tischenko et al. [2006] pointed out nitrite maximum, which is an indirect evidence of denitrification, near the bottom.

In general, denitrification is occurred in the restricted condition that oxygen is absent or very low concentrations, and reduces N/P ratio because nitrate is used as oxidant instead of O2 [Anderson and Sarmiento, 1994]. Ironically, the East Sea is well known as high oxygen condition in the northern Pacific Ocean, because it has own water formation system [Kim et al., 1996; Talley et al., 2006]. Considered it in relation to the recent changes of the East Sea, however, some phenomena seem to be related to biogeochemical change.

Here, we will therefore deal with some symptoms that are suspected as a result of denitrification, despite high oxygen condition, estimate the amount of denitrification by linear

mixing inverse model including biogeochemical changes, and construct a feedback loop based on the previous literatures that reported warming evidences in the East Sea.

2. Material and Method

2.1 Data

In 1999, two cruises were carried out enough to cover the whole East Sea for summer, except for the territorial waters of North Korea [Fig. 1]. The project, which is shortly named as CREAMS (Circulation Research of East Asian Marginal Seas)Ⅱ, was firstly collaborated by three countries: United States, Russia, and South Korea. More specific cruise information is available in Talley et al. [2004], and the source of data used is from *http://sam.ucsd.edu/onr_data/hydrography.html*.

The East Sea has three basins: Japan Basin (JB), Ulleung Basin (UB), and Yamato Basin (YB). As shown in Fig. 1, to facilitate the presentation of our analysis we have further divided the Japan Basin at 135E into the Western Japan Basin (WJB) and the Eastern Japan Basin (EJB).

2.2 Method

Originally, Tomczak and Large [1988] developed the OMP analysis, not considering biogeochemical changes. Then, Karstensen and Tomczak [1998] introduced extended OMP analysis including the redfield ratio to involve biogeochemical changes. Again, To assess

remineralization, dentrification and carbonate behaviors, Hupe and Karstensen [2000] more improved the extended OMP analysis to be able to assess not only mixing process, but also advanced biogeochemical changes such as remineralization, dentrification and carbonate behaviors. Therefore, we applied further extended Optimum Parameter (OMP) analysis by Hupe and Karstensen [2000] to estimate denitrification in the East Sea.

2.2.1 Model equations

More details are given by Hupe and Karstensen [2000]. Here, we will explain in brief.

The matrix form of linear inverse mixing model is written as:

$$\begin{bmatrix} T_1 & \cdots & T_4 & 0 & 0 & 0 \\ S_1 & \cdots & S_4 & 0 & 0 & 0 \\ DO_1 & \cdots & DO_4 & r_{O2/P} & 0 & 0 \\ P_1 & \cdots & P_4 & 1 & r_D & 0 \\ N_1 & \cdots & N_4 & r_{N/P} & 1 & 0 \\ Si_1 & \cdots & Si_4 & r_{Si/P} & 0 & 0 \\ TALK_1 & \cdots & TALK_4 & -r_{N/P} & 1 & 2 \\ DIC_1 & \cdots & DIC_4 & r_{Corg/P} & r_D r_{Corg/P} & 1 \\ 1 & \cdots & 1 & 0 & 0 & 0 \end{bmatrix} \times \begin{bmatrix} x_1 \\ x_2 \\ x_3 \\ x_4 \\ \Delta P \\ \Delta N^{deni} \\ \Delta C_{inorg} \end{bmatrix} - \begin{bmatrix} T_{obs} \\ S_{obs} \\ DO_{obs} \\ P_{obs} \\ N_{obs} \\ Si_{obs} \\ TALK_{obs} \\ DIC_{obs} \\ 1 \end{bmatrix} = \begin{bmatrix} R_T \\ R_S \\ R_{DO} \\ R_P \\ R_N \\ R_{Si} \\ R_{TALK} \\ R_{DIC} \\ R_{MC} \end{bmatrix}$$

$$\mathbf{A} \times \boldsymbol{x} - \boldsymbol{d} = \mathbf{R}$$

A matrix on the left-hand side is defined as the source water types, and T, S, DO, P, N, Si, TALK, and DIC denote temperature, salinity, dissolved oxygen, phosphate, nitrate, silicate, total alkalinity, and dissolved inorganic carbon, respectively. The numbers of $r_{tracers/P}$ are composed of the redfiled ratios. The first column is composed of mixing ratios of x_i between water

masses, remineralized phosphate of ΔP from organic matters, denitrification of ΔN^{deni}, inorganic carbon of ΔC_{inorg} by dissolution of calcareous material. The second column is the observed data, $T_{obs},\ldots,DIC_{obs}$, and the last represents residual column deviated from solutions. The last row is to constrain one that is the sum of x_i. This equation is based on an over-determined system, and solved by weighted nonnegative least squares (NNLS) method as follows:

$$R^T R = (Ax-d)^T W^T W (Ax-d) = \sum_{j=1}^{m} W_j^2 \left(\sum_{i=1}^{n} A_{ji} x_i - d_j \right)^2$$

The characteristics of source water types and weight values assigned for the tracers are summarized in Table 2.

2.2.2 Redfield Ratios

The traditional composition of marine phytoplankton organic matter is expressed as:

$$106CO_2 + 16HNO_3 + H_3PO_4 + 122H_2O$$
$$\Leftrightarrow (CH_2O)_{106}(NH_3)_{16}(H_3PO_4) + 138O_2$$

The stoichiometric ratios of C:N:P:O_2 of 106:16:1:-138 are named as Redfield ratio developed by A.C. Redfield [Redfield et al., 1963]. These ratios appeared broadly constant value in the world oceans. However, more recent observations indicated that the Redfield ratio was needed to revise. Recently, Anderson and Sarmiento [1994] reexamined Redfield rations through the remineralization in deep oceans below 400m, and suggested the revised number of C:N:P:O_2 of

117±14:16±1:1:-170. One year later, Anderson [1995] reanalyzed the mean composition of the primary components of phytoplankton organic matter in the surface ocean, and revised the Redfield ratio such as 106:16:1:151±10. The Redfield ratio in the East Sea was much different number with the traditional and revised Redfield ratios, and estimated as C:N:P:O2 = 106:12.4:1:-117.

Hence, we applied the representative numbers of Redfield ratios above to our modeling to validate our results. Silicate is not directly connected to the remineralization of particulate organic matter, so that the number for $r_{si/P}$ is cited from Hupe and Karstensen [2000]. The $r_{si/P}$ of the East Sea is estimated as 37/1. The modeling was carried out according to each case using different Redfield ratio, and the ratios used are summarized in Table 3.

3. Results and Discussion

3.1 Implication of biogeochemical change

Density field in the East Sea showed constant feature below depth of 300m with latitude [Kim and Lee, 2006]. Thus, not to consider the influence of seasonal variation, the data below 300m in depth were analyzed, except for Fig. 4b.

In the Fig. 2a, the N/P ratio of the East Sea is estimated about 12.4 by the least square fit, and is much lower than the Redfield ratio of 16. Apparently, this means that the East Sea plays a

significant role as N – sink region in global oceans. However, we have not any evidence to support the fact so far. As shown in Fig. 2b zoomed in the dotted lines of Fig. 2a, it found that some data are deviated from the fitted line. These indicate the fact that nitrate loss occurs in the East Sea, especially, in the Ulleung Basin.

As a result of nitrate loss, intense N/P ratio minimum zone exists between 900m and 2200m in the Ulleung Basin [Fig. 3a]. Dissolved oxygen profile of Fig. 3b also shows minimum concentrations at the same zone, and nitrite, which is an intermediate product by denitrification, is detected [Fig. 3c]. Nitrite is a useful indicator to determine oxidative or reductive pathway in the nitrogen cycle [Lomas and Lipschultz, 2006]. Generally, the primary maximum peak is produced by nitrification ($NH_4^+ \rightarrow NO_2^- \rightarrow NO_3^-$) in the euphotic zone, and the secondary peak below the euphotic zone is due to denitrification ($NO_3^- \rightarrow NO_2^- \rightarrow N_2O/N_2$). Hence, Fig. 3c should be connected with the reductive pathway.

Fig. 4 shows precise structures of two representative stations, which are thought be as the strong candidates expecting the occurrence of denitrification within the Ulleung Basin. The station 10 is located in continental slope, and the station 27 is in basin [Fig. 4a]. The profiles of nitrate of two stations follow typical pattern in comparison with open oceans: that is, nitrate concentrations at the surface are very low, and then are rapidly increased near thermocline depths due to remineralization [Fig. 4b]. The profiles below the thermocline depths are seemed

to be not significant variation. However, as zoomed in deeper than depth of 300m, dynamic profiles different from the previous those are found [Fig. 4c]. The nitrate profile of station 10 is slightly reversed near the bottom [Fig. 4c], simultaneously DO concentrations are steeply decreased, nitrite is detected [Fig. 4d], and N/P ratio is drastically dropped [Fig. 4f]. These results are mostly confined near the bottom.

Also, the reversed profile is found at depth of 1800m of station 27 [Fig. 4c]. Concurrently nitrite shows a peak at 1800m, oxygen consumption is little because nitrate instead of oxygen was used as oxidant [Fig. 4e], and the number of N/P ratio is less than 12.4 [Fig. 4f]. The reversed shape at the station 27 exists near the bottom [Fig. 4c], but nitrite is not detected [Fig. 4e]. The consequences of station 27 seem to be different from the station 10 - that is, the reversed depth of station 27 is far about 400m from the bottom, and the nitrite maximum at the station 10 shows near the bottom; on the other hand, that of the station 27 appears in water column.

When occurred denitrification, nitrate concentrations are necessarily decreased because nitrate instead of oxygen is used to oxidize organic matter under low oxygen content. Specifically, the case of station 10 is seemed to be close to benthic denitrification, and the station 27 is definitely the typical case of water denitrification. Obviously, the results of two stations imply important evidences that denitrification is occurring in the East Sea, especially, in

the Ulleung Basin. However, we have to note the fact that the East Sea is still plentiful in oxygen compared with the condition denitrified; for example, oxygen concentrations in the Arabian Sea are almost zero (< 5 $\mu mol \cdot kg^{-1}$) near the oxygen minimum zone [Hupe and Karstensen, 2000]. As considered the recently drastic changes of the East Sea, we think that the phenomenon might be responsible for biogeochemical change driven by global warming.

Therefore, as the next step, we are going to quantify the amount of denitrification in the East Sea through a suitable model.

3.2 Estimation of denitrification by the linear inverse model

The Fig. 5 shows the stations that denitrification estimated by the linear inverse model is greater than zero according to each case applied by the different number of Redfield ratio. Even though some stations are distributed near the Tatar Straight in the EJB and in the middle of WJB [Fig. 5a and 5c], most of stations are concentrated in the UB. The Fig. 6 appears the common stations extracted from the four cases.

The levels of denitrificatoin estimated in the four cases are ranged from about 50 to 450 $\mu mol \cdot m^{-3}$ [Fig. 7]. All cases show the min value at the station of 27 and the max value at the station of 17 in common. To estimate the flux of denitrification needs to involve time unit. Thus, we use a concept of pseudo-age, using oxygen utilization rate (OUR) [Poole and Tomczak, 1999]. The idea is expressed as:

$$pseudo-age(year)=\frac{AOU(\mu mol\cdot kg^{-1})}{OUR(\mu mol\cdot kg^{-1}\cdot year^{-1})}$$

, where the term of apparent oxygen utilization (AOU) is calculated:

$$AOU=[O_2]_{saturation}^{T,S,P}-[O_2]_{observed}$$

Recently, the OUR value of the East Sea was reported by Min [1999] from CFCs data and Kim et al. [2003] from moving boundary box model (MBBM), and summarized in Table 4. Thus, the flux is estimated by the combination of pseudo-age, the profile of $\Delta N^{deni}\left(\mu mol\cdot m^{-3}\right)$, and area calculated from the bottom to a certain depth greater than zero of ΔN^{deni}. The process is illustrated in the Fig. 8 in details.

The flux of denitrification based on CFCs is ranged from 4 to 18 $\mu mol\cdot m^{-2}\cdot day$, and the level is high around the station of 19 and 120 [Fig. 9]. Also, the results linked to MBBM show a similar range that is from 8 to 25 $\mu mol\cdot m^{-2}\cdot day$, and the distribution is overall consistent with those of CFCs, even though the flux level around the station of 17 is higher from MBBM than that from CFCs [Fig. 10]. The mean flux of denitrification in the UB is estimated as 9.0 ~ 16.0 $\mu mol\cdot m^{-2}\cdot day$ [Table 5]. It is found from the two results that the flux of denitrification is high near the edge of continental slope.

To estimate the denitrification rate within the boundary of common stations we need to know the boundary area. So, it is composed of the grid lines that connect each box known in size, and then counts how many boxes are included in the boundary area [Fig. 11]. The

boundary area is approximately estimated of $7.0926 \times 10^3 km^2$. Therefore, the mean denitrification rate is ranged from $6.38 \times 10^4 \sim 11.35 \times 10^4 mol \cdot d^{-1}$. In addition, our estimation of denitrification was well comparable to the experimental result from incubated sediment [personal communication with Prof. An].

3.3 Expectation of a feedback loop based on biogeochemical changes

Although the present denitrification of the East Sea is not significant level compared with the major areas, for examples, Arabian Sea and eastern equatorial Pacific, where are known to occur actively denitrification due to the existence of oxygen minimum zone (OMZ), we need to note that the evidences so far are supporting that the East Sea is occurring denitrification, though high oxygen content.

We think two reasons why it is possible to occur denitrification in high oxygen environment. One is that this might be regarded as a new founding unknown, because denitrification is known as that it is occurred only in low oxygen condition. Another reason is supposed by increased temperature in deep sea. Denitrifying bacteria are very sensitive to temperature change; that is, positive relationship with temperature.

We regard the latter as the main reason, rather than the former. In deep sea, temperature has been maintained constantly by density stability, so that the bacteria have been adapting the constant temperature for a long time. The recent investigations are reporting not only the

increase in surface temperature, but also in the deep temperature.

Hence, we can expect a feedback loop with respect to biogeochemical change. If the global warming accelerates continuously, water formation is decreased [Gamo, 1999; Gamo et al., 2001; Kang et al., 2003b; Chae et al., 2005; Postlethwaite et al., 2005] as sea surface temperature (SST) increases [Gamo, 1999; Min and Kim, 2006], and then low oxygen environment is enhanced [Kim and Kim, 1996; Chen et al., 1999; Kim et al., 2001; Kang et al., 2004; Kim et al., 2004]. This enforces will increase in denitrification. It is a source to produce nitrous oxide (N_2O), which is well known as greenhouse gas, and nitrous oxide is released from ocean to atmosphere.

Consequently, we expect that these processes will operate as a positive feedback in the future [Fig. 12], if otherwise the global warming soothes. We think that this matter is also supposed to stimulate special curiosity to other oceanographic scientists, and feel that more extended analysis is needed to find out the recent changes of the East Sea.

Acknowledgements

I would like to thank Prof. Zong-Liang Yang for valuable teaching. This paper used the CREAMS Ⅱ hydrographic data, and was to do homework for the class of physical climatology.

References

Anderson,, L. A. 1995. On the hydrogen and oxygen content of marine phytoplankton. *Deep-Sea Res.. Ⅰ*, 42, 1675-1680.

Anderson, L.A. and J.L. Sarmiento. 1994. Redfield ratios of remineralization determined by nutrient data analysis. *Global Biogeochem. Cycles*., 8(1), 65-80.

Chae, Y.K., Y.H. Seung, and S.K. Kang. 2005. Mode change of deep water formation deduced from slow variation of thermal structure: one-dimensional model study. *Ocean and Polar Research*., 27(2), 115-123. (in Korean)

Chen, C.-T.A., G..-C. Gong, S.-L. Wang, and A.S. Bychkov. 1996. Redfield ratios and regeneration rates of particulate matter in the Sea of Japan as a model of closed system. *Geophysical Research Letter*., 23(14), 1785-1788.

Chen, C.-T.A., A.S. Bychkov, S.L. Wang, and G.Yu. Pavlova. 1999. An anoxic Sea of Japan by the year 2200?. *Marine Chemistry*., 67, 249-265.

Chung, C.S., J.H. Shim, Y.C. Park, and S.G.. Park. 1989. Primary productivity and nitrogenous nutrient dynamics in the East Sea of Korea. *Journal of the Korean Society of Oceanography.*, 24, 52-61. (in Korean)

Gamo, T. 1999. Global warming may have slowed down the deep conveyor belt of a marginal sea of the northwestern Pacific: Japan Sea. *Geophysical Research Letters.*, 26, 3137-3140.

Gamo, T., N. Momoshima, and S. Tolmacheyov. 2001. Recent upward shift of the deep convection system in the Japan Sea, as inferred from the geochemical tracers tritium, oxygen, and nutrients. *Geophysical Research Letters.*, 28(21), 4143-4146.

Hupe, A. and J. Karstensen. 2000. Redfield stoichiometry in Arabian Sea subsurface waters. *Global Biogeochem. Cycles*., 14(1), 357-372.

Kang, D.-J., K.-E. Lee, and K.-R. Kim. 2003a. Recent development in chemical oceanography of the East (Japan) Sea with an emphasis on CREAMS finding: A review. *Geosciences Journal*., 7(2), 179-197.

Kang, D.-J., S. Park, Y.-G. Kim, K. Kim, and K.-R. Kim. 2003b. A moving-boundary box model (MBBM) for oceans in change: An application to the East/Japan Sea. *Geophysical Research Letters.*, 30(6), 1299, doi:10.1029/2002GL016486.

Kang, D.-J., J.-Y. Kim, T. Lee, and K.-R. Kim. 2004. Will the East/Japan Sea become an anoxic sea in the next century ? *Marine Chemistry*., 91, 77-84.

Karstensen, J., M. tomczak. 1998. Age determination of mixed water masses using CFC and oxygen data. *J. Geophys. Res*., 109, 18599-18610.

Kido, K. and M. Nishimura. 1973. Regeneration of silicate in the Ocean. Ⅰ. The Japan Sea as a model of a closed system. *J. Oceanogr. Soc. Japan*., 29, 185-192.

Kim, I.-N. and T. Lee. 2004. Summer hydrographic features of the East Sea analyzed by the Optimum Multiparameter method. *Ocean and Polar Research*., 26(4), 581-594. (in Korean)

Kim, I.-N. and T. Lee. 2006. Properties of the East Sea Intermediate Water revealed by isopycnal analysis. Proceedings of the autumn meeting 2006 of the Korean Society of Oceanography., 373.

Kim, J.-Y., D.-J. Kang, E, Kim, J.H. Cho, C.R. Lee, K.-R. Kim, and T. Lee. 2003. Biological pump in the East Sea estimated by a box model. *Journal of the Korean Society of Oceanography.*, 8(3), 295-306. (in Korean)

Kim, K.-R. and K. Kim. 1996. What is happening in the East Sea (Japan Sea) ?; Recent chemical observations during CREAMS 93-96. *Journal of the Korean Society of Oceanography.*, 31(4), 164-172.

Kim, K., K.-R. Kim, D. Min, Y. Volkov, J.-H. Yoon, and M. Takematsu. 2001. Warming and Structural Changes in the East Sea(Japan Sea): A clue to future changes in Global Oceans? *Geophysical Research Letters.*, 28, 3293-3296.

Kim, K., K.-R. Kim, Y.-G. Kim, Y.-K. Cho, D.-J. Kang, M. Takematsu, and Y. Volkov. 2004. Water masses and decadal variability in the East Sea (Sea of Japan). *Progress in Oceanography*., 61, 157-174.

Kim, K., K.-R. Kim, Y.G. Kim, Y.K. Cho, J.Y. Chung, B.H. Choi, S.K. Byun, G.H. Hong, M. Takematsu, J.H. Yoon, Y. Volkov, and M. Danchenkov, 1996. New findings from CREAMS Observation: Water Masses and Eddies in the East Sea. *Journal of the Korean Society of Oceanography.*, 31(4), 155-163.

Lomas, M.W. and F. Lipschultz. 2006. Forming the primary nitrite maximum: Nitrifiers or phytoplankton ? *Limnol Oceanogr*., 51(5), 2453-2467.

Min, D.-H. and M.J. Warner. 2005. Basin-wide circulation and ventilation study in the East Sea (Sea of Japan) using chlorofluorocarbon tracers. *Deep Sea Research II*, 52(11-13), 1580-1616.

Min, H.S. and C.-H. Kim. 2006. Water mass formation variability in the intermediate layer of the East Sea. *Ocean Science Journal*., 41(4), 255-260.

Moon, C.H., H.S. Yang, and K.W. Lee. 1996. Regeneration Processes of nutrients in the Polar Front Area of the East Sea Ⅰ. Relationship between Water Mass and nutrient Distribution Pattern in Autumn. *J. Korean Fish. Soc*., 29(4): 503-526. (in Korean)

Nicholls, J.C., C.A. Davies, and M. Trimmer. 2007. High-resolution profiles and nitrogen isotope tracing reveal a dominant source of nitrous oxide and multiple pathways of nitrogen gas formation in the central Arabian Sea. *Limnol Oceanogr*., 52(1), 156-168.

Poole, R. and M. Tomczak. 1999. Optimum multiparameter analysis of the water mass structure in the Atlantic Ocean thermocline. Deep-Sea Res. Ⅰ., 46, 1895-1921.

Postlethwaite, C.F., E.J. Rohling, W.J. Jenkins, and C.F. Walker. 2005. A tracer study of ventilation in the Japan/East Sea. *Deep-Sea Research II*, 52, 1684-1704.

Redfield, A.C., B.H. Ketchum and F.A. Richards. 1963. The influence of organism on the composition of sea water, in The sea., 2, 26-77.

Seung, Y.H. and K. Kim. 1997. Estimation of the residence time for renewal of the East Sea Intermediate Water using MICOM. *Journal of the Korean Society of Oceanography.*, 32(1), 17-27.

Shim, J.H., S.R. Yang, and W.H. Lee. 1989. Phytohydrography and the vertical pattern of nitracline in the southern waters of the Korean East Sea in early spring. *Journal of the Korean Society of Oceanography.*, 24, 15-28.

Talley, L.D., D.-H. Min, V.B. Lobanov, V.A. Luchin, V.I. Ponomarev, A.N. Salyuk, A.Y. Shcherbina, P.Y. Tishchenko, and I. Zhabin. 2006. Japan/East Sea water masses and their relation to the sea's circulation. *Oceanography*., 19(3), 32-49.

Talley, L.D., P. Tischenko, V. Luchin, A. Nedashkovskiy, S. Sagalaev, D.-J. Kang, M. Warner, and D.-H. Min. 2004. Atlas of Japan (East) Sea hydrographic properties in summer, 1999. *Progress in Oceanography*., 61, 277-348.

Tishchenko, P.Y., L.D. Talley, V. Labanov, A. Nedashkovskiy, M. Shvetsova, and S. Sagalaev. 2006. Impact of geochemical processes on hydrochemical properties of the Japan Sea. Submitted to *Oceanology*. (in Russian)

Tomczak, M. and D.G.B. Large. 1989. Optimum Multiparameter analysis of mixing in the thermocline of the Eastern Indian Ocean. *Journal of Geophysical Research.*, 94, 16141-16149.

Yanagi, T., 2002. Water, salt, phosphorus and nitrogen budgets of the Japan Sea. *Journal of Oceanography*., 58, 797-804.

Yang, H.S., S.S. Kim, C.G. Kang, and K.D. Cho. 1991. A study on sea water and ocean current in the sea adjacent to Korea Peninsula. Ⅲ. Chemical characteristics of water masses in the polar front area of the central Korean East Sea. *J. Korean Fish. Soc*., 24(3), 185-192. (in Korean)

Figure Captions

Fig. 1. Map showing the hydrographic stations and topography of the East Sea. The East Sea shows dynamical topography that is consisted of three basins; JB (Japan basin), YB (Yamato Basin), and UB (Ulleung Basin), one rise; YR (Yamato Rise), and four straits; KR (Korea Strait), TS (Tsugaru Strait), ST (Soya Strait), and TtS (Tatar Strait). To facilitate our presentation analysis, the Japan Basin at 135°E is divided into the Western Japan Basin (WJB) and the Eastern Japan Basin.

Fig. 2. N:P ratio of the East Sea below depth of 300m. a) The number of N/P ratio is estimated by least square method, and is simultaneously plotted with the traditional Redfield ratio of 16, b) The area within the dotted lines is zoomed.

Fig. 3. The vertical distributions of N/P ratio, dissolved oxygen, and nitrite in the East Sea. Each color represents each basin as follos: red circle of Western Japan Basin, green circle of Eastern Japan Basin, blue circle of Ulleung Basin, and pink circle of Yamato Basin. a) N/P ratio, b) dissolved oxygen (μmol/kg), c) nitrite (μmol/kg).

Fig. 4. Representations of the two stations that are strongly expected to occur denitrification in the Ulleung Basin. a) Locations of the two stations on map, b) The vertical profiles of nitrate, c) The nitrate profiles zoomed in below depth of 300m, d) The vertical profiles of dissolved oxygen and nitrite of the station 10, e) The vertical profiles of dissolved oxygen and nitrite of the station 27, f) The N/P ratio profiles of the two stations.

Fig. 5. Stations that might occur denitrification expected by the linear inverse model.

Fig. 6. The common locations extracted from the four cases.

Fig. 7. Vertical profiles of denitrification (ΔN^{deni}) estimated by the linear inverse model. Gray line means bottom depth of each station.

Fig. 8. An illustration of calculation for pseudo-age concept.

Fig. 9. The horizontal distributions of denitrification flux ($\mu mol \cdot m^{-2} \cdot day^{-1}$) based on CFCs [Min, 1999].

Fig. 10. The horizontal distributions of denitrification flux ($\mu mol \cdot m^{-2} \cdot day^{-1}$) based on MBBM [Kim et al., 2003].

Fig. 11. The estimation of boundary area from the grid boxes.

Fig. 12. A loop of biogeochemical feedback expected in the East Sea.

Table Captions

Table 1. A summary of the previous results on the number of N/P ratio of the East Sea.

Table 2. The characteristics of source water types and weight values assigned for the tracers

[Kim and Lee, 2004].

Table 3. The Redfield ratios used for the modeling.

Table 4. OUR values of the Ease Sea reported by Min [1999] and Kim et al. [2003].

Table 5. The flux of denitrification estimated by the linear inverse model.

Fig. 1

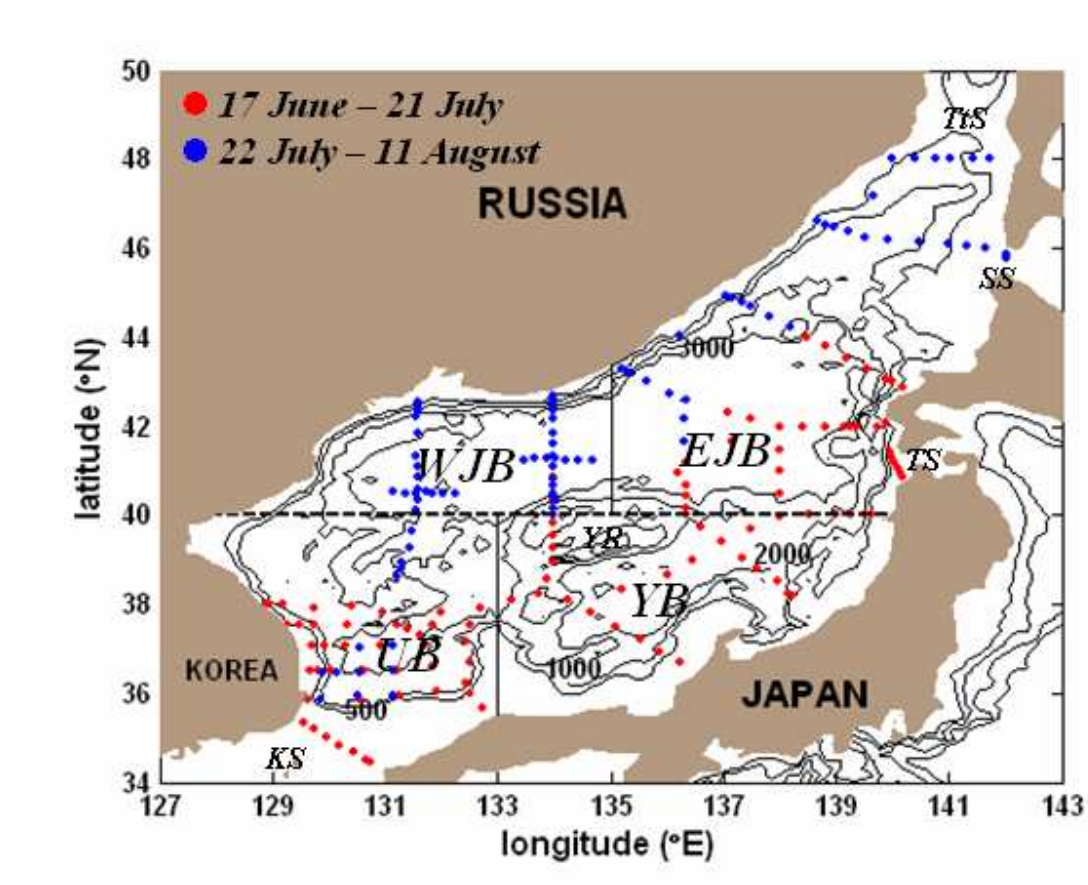
17 June – 21 July
22 July – 11 August
RUSSIA
KOREA
JAPAN
WJB
EJB
UB
YB
YB
TtS
SS
TS
KS
3000
2000
1000
500
latitude (°N)
longitude (°E)

Fig. 2

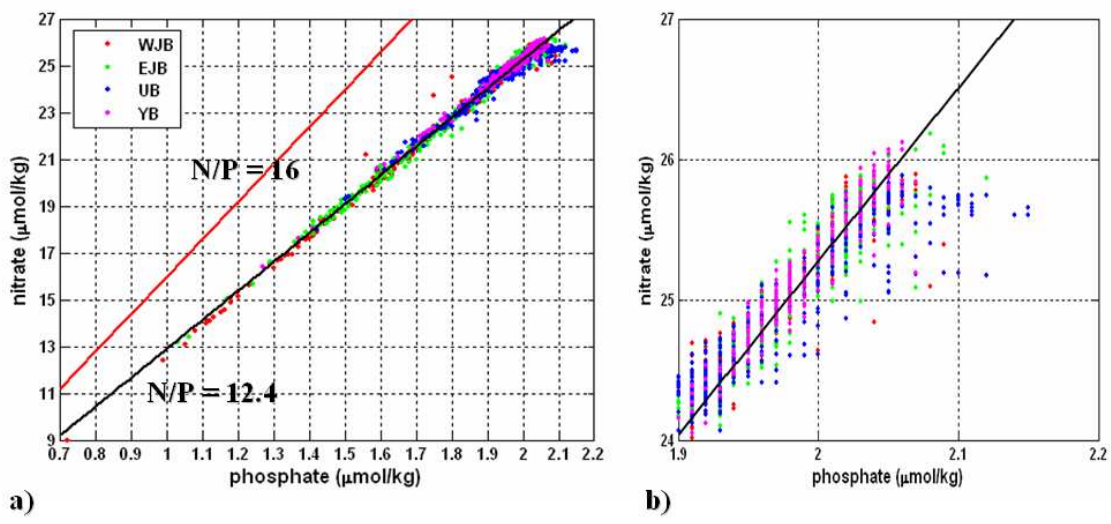
WJB
EJB
UB
YB
N/P = 16
N/P = 12.4
nitrate (μmol/kg)
phosphate (μmol/kg)
a)
b)

Fig. 3

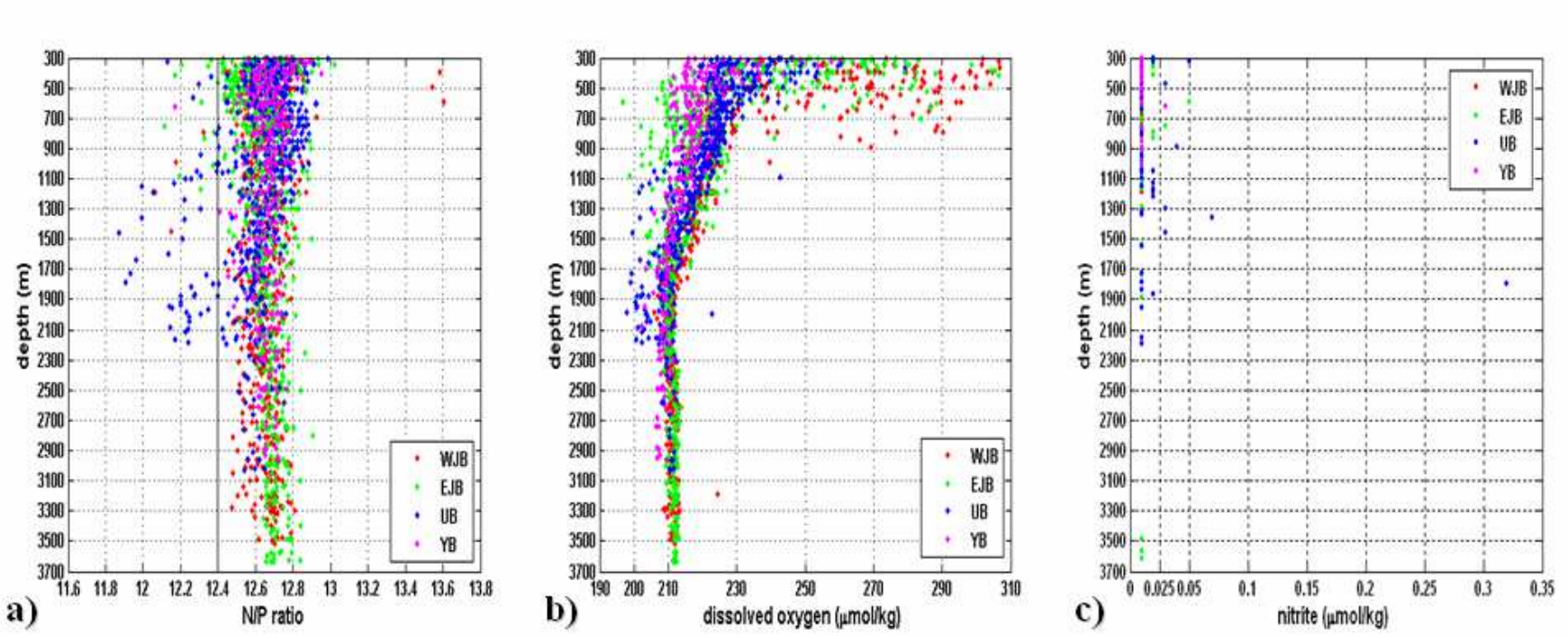
a)
depth (m)
N/P ratio
WJB
EJB
UB
YB
b)
depth (m)
dissolved oxygen (μmol/kg)
WJB
EJB
UB
YB
c)
depth (m)
nitrite (μmol/kg)
WJB
EJB
UB
YB

Fig. 4

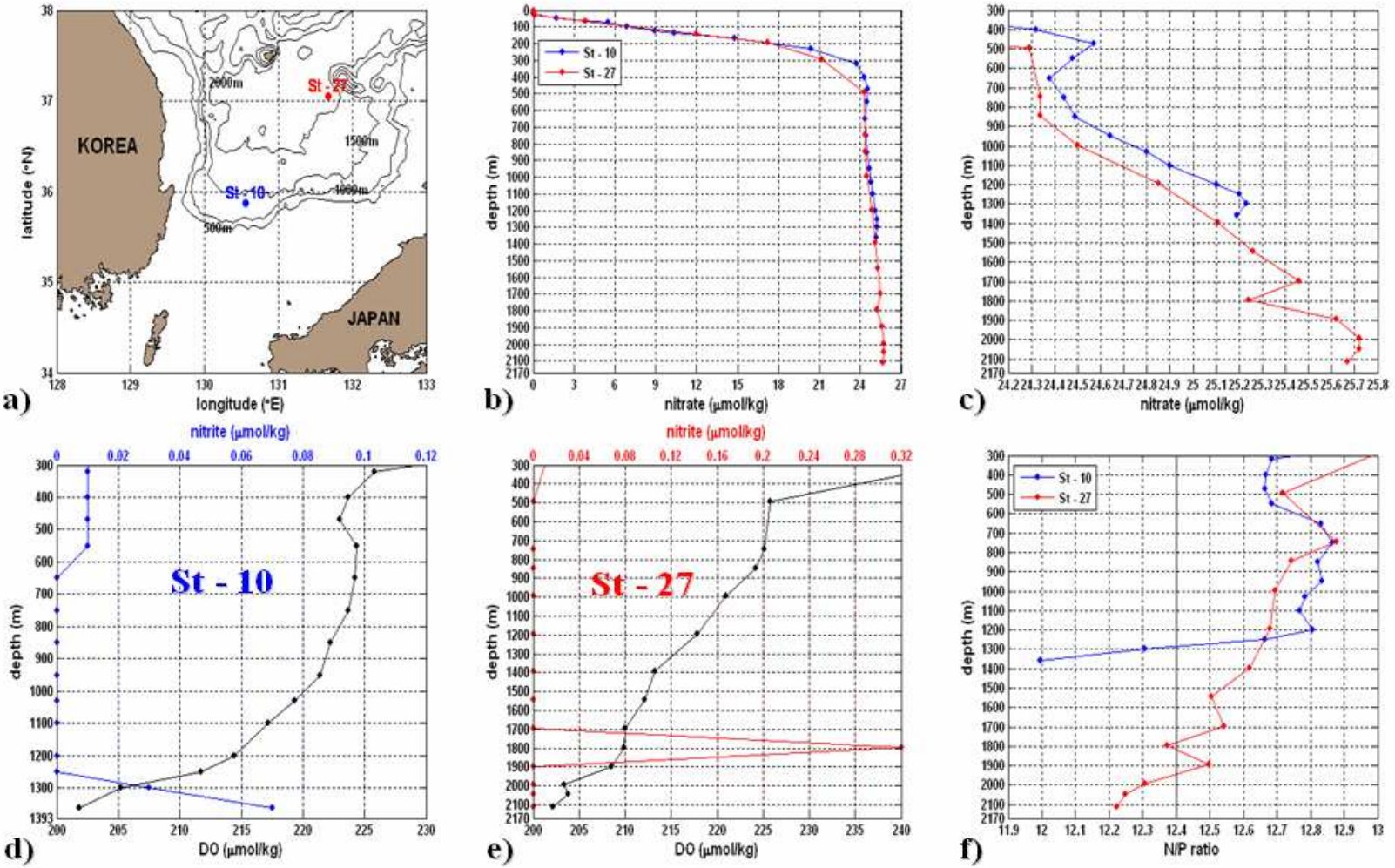
a)
KOREA
JAPAN
St - 27
St - 10
2000m
1500m
1000m
500m
latitude (°N)
longitude (°E)
b)
St - 10
St - 27
depth (m)
nitrate (μmol/kg)
c)
depth (m)
nitrate (μmol/kg)
d)
nitrite (μmol/kg)
St - 10
depth (m)
DO (μmol/kg)
e)
nitrite (μmol/kg)
St - 27
depth (m)
DO (μmol/kg)
f)
St - 10
St - 27
depth (m)
N/P ratio

Fig. 5

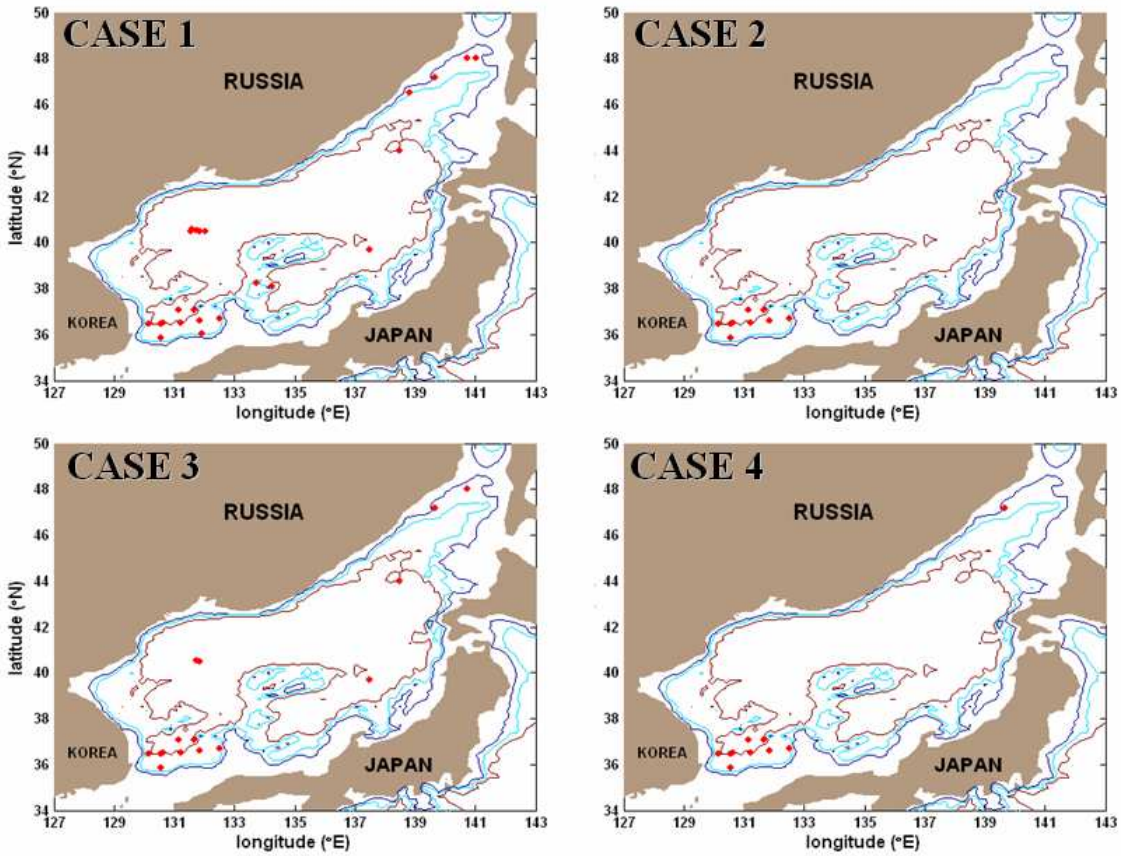
CASE 1
CASE 2
CASE 3
CASE 4
RUSSIA
KOREA
JAPAN
latitude (°N)
longitude (°E)

Fig. 6

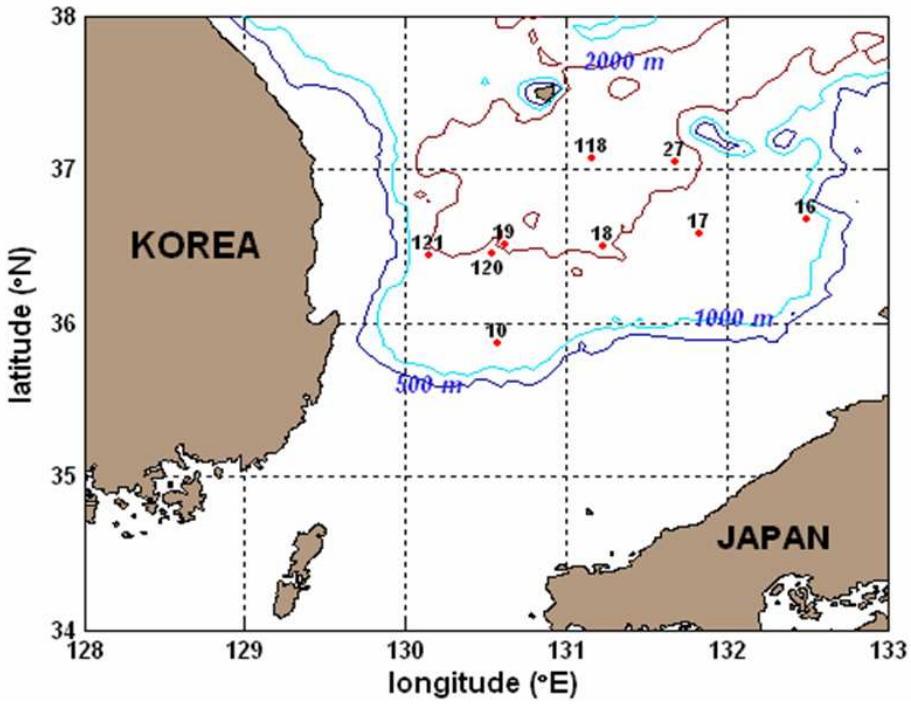
KOREA
JAPAN
2000 m
1000 m
500 m
118
27
16
17
18
19
121
120
10
latitude (°N)
longitude (°E)

Fig. 7

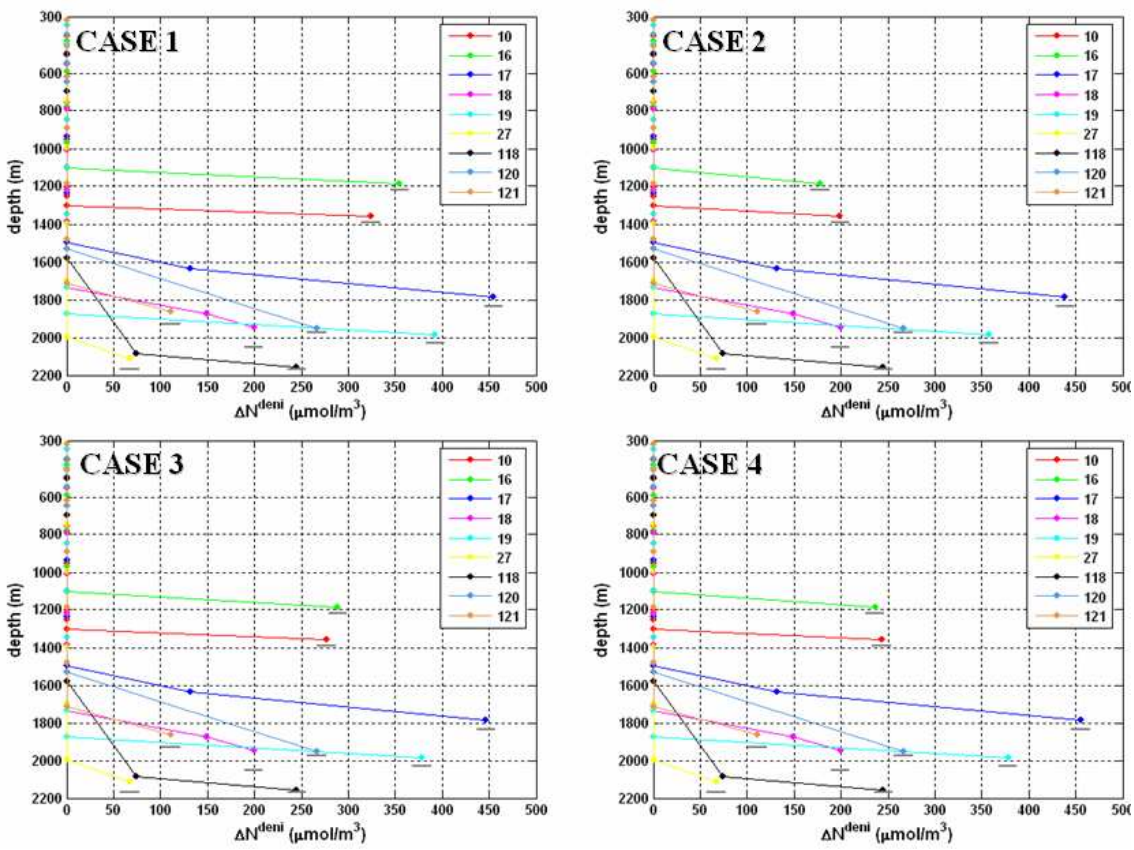

Fig. 8

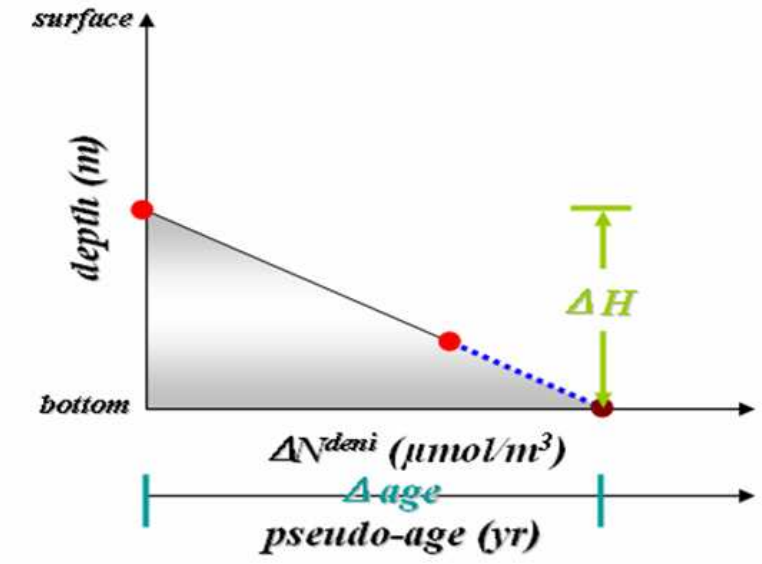

$$\Rightarrow \; denitrification = \frac{\Delta N^{deni} \times \Delta H}{2 \cdot \Delta age \cdot 365} \left(\frac{\mu mol}{m^2 \cdot day} \right)$$

Fig. 9

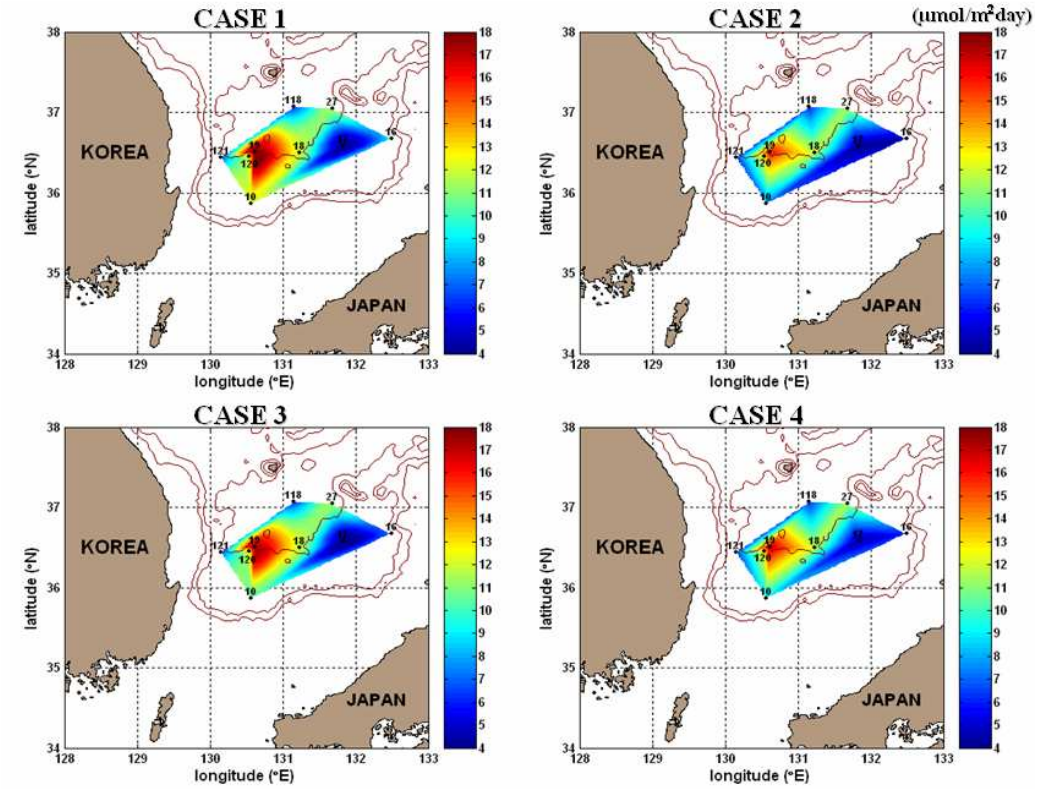
CASE 1
CASE 2
CASE 3
CASE 4
(μmol/m²day)
KOREA
JAPAN
latitude (°N)
longitude (°E)

Fig. 10

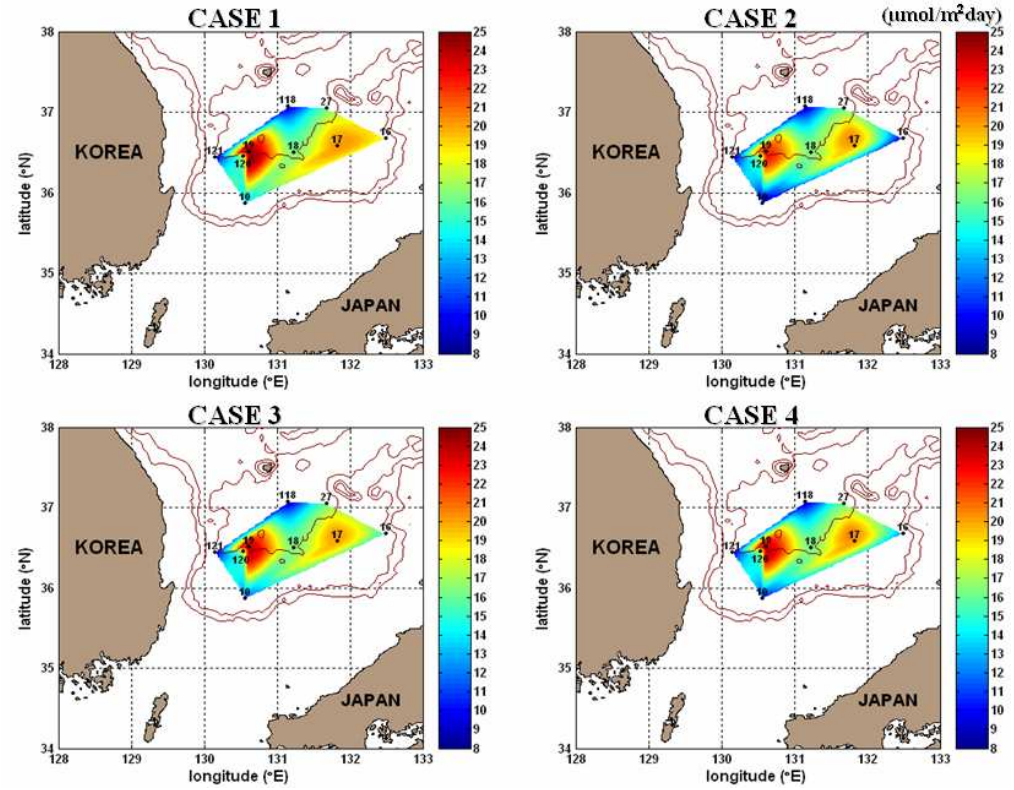
CASE 1
CASE 2
CASE 3
CASE 4
(μmol/m²day)
KOREA
JAPAN
latitude (°N)
longitude (°E)

Fig. 11

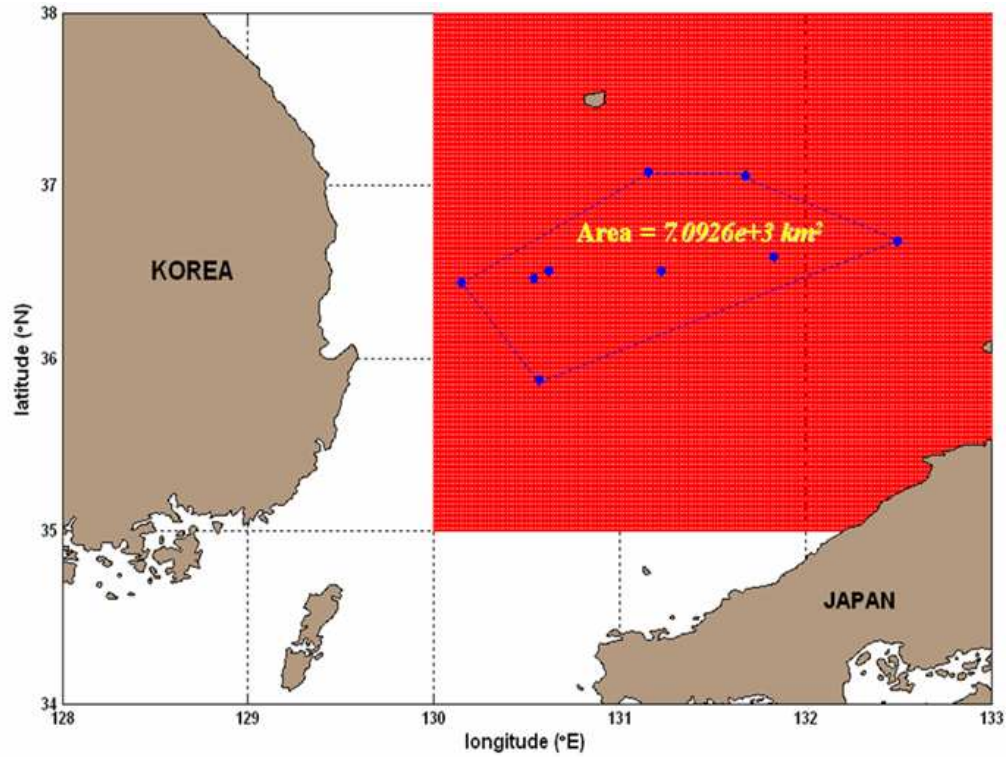
Area = 7.0926e+3 km²
KOREA
JAPAN
latitude (°N)
longitude (°E)
38
37
36
35
34
128
129
130
131
132
133

Fig. 12

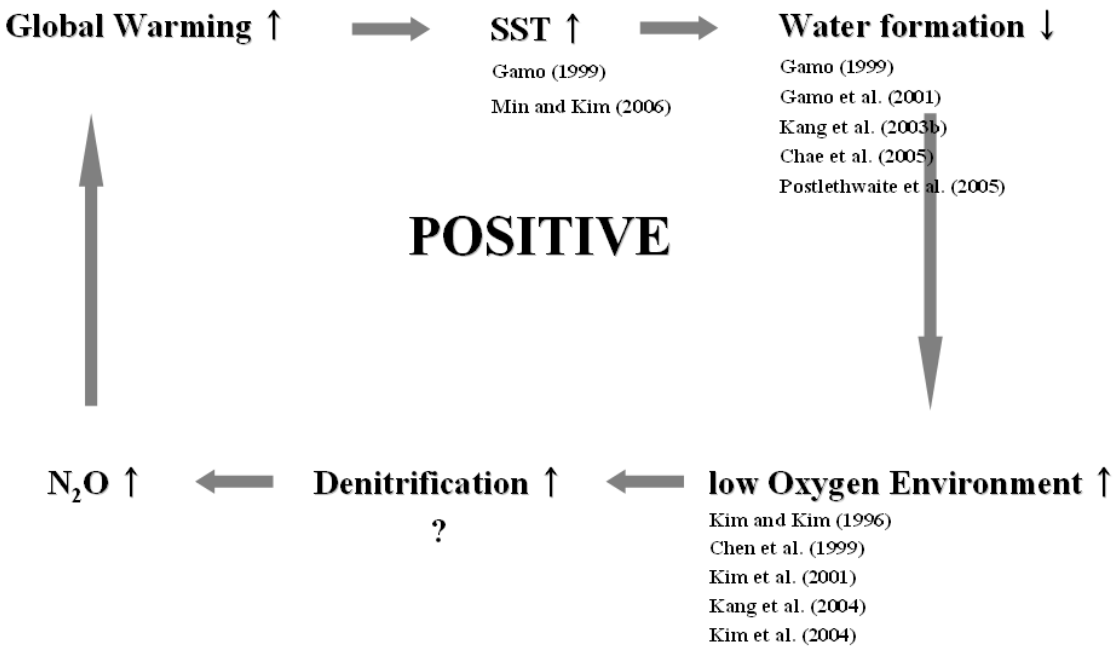
Global Warming ↑
SST ↑
Gamo (1999)
Min and Kim (2006)
Water formation ↓
Gamo (1999)
Gamo et al. (2001)
Kang et al. (2003b)
Chae et al. (2005)
Postlethwaite et al. (2005)
POSITIVE
N2O ↑
Denitrification ↑
?
low Oxygen Environment ↑
Kim and Kim (1996)
Chen et al. (1999)
Kim et al. (2001)
Kang et al. (2004)
Kim et al. (2004)

Table 1.

N : P ratio				
Source	**Whole (W/EJB + UB + YB)**	**lat < 40°N (UB + YB)**	**lat ≥ 40°N (W/EJB)**	**season**
This study	12.40			summer
Kido and Nishimura (1973)	13.60	-	-	summer
Shim et al. (1989)	-	12.54	-	spring
Chung et al. (1989)	-	13.41	-	fall
Yang et al. (1991)	-	12.10	-	fall
Moon et al. (1996)	-	14.36	-	fall
Chen et al. (1996)	14.70 (300m ~ 600m)			
	13.00 (≥2000m)			
Yanagi (2002)	11.30	-	-	annual
Kang et al. (2003a)	12.80 (WJB+UB)	-	-	summer
Total range	**11.30 ~ 14.70**			

Table 2.

	T (℃)	S (‰)	DO (μmol·kg^{-1})	P (μmol·kg^{-1})	N (μmol·kg^{-1})	Si (μmol·kg^{-1})	TALK (μmol·kg^{-1})	DIC (μmol·kg^{-1})
[1]TMW	19.528	34.504	219.1	0.17	0.85	2.90	2281.6	2045.8
[2]LCW	1.742	33.829	352.6	0.45	3.61	6.20	2262.6	2217.0
[3]ESIW	1.436	34.042	319.7	0.91	11.44	16.80	2264.5	2253.9
[4]ESPW	0.175	34.065	198.8	2.12	25.86	89.40	2284.6	2369.2
Weight value	142	142	97	43	47	65	4	1

[1]TMW: Tsushima Middle Water, [2]LCW: Liman Cold Water, [3]ESIW: East Sea Intermediate Water, [4]ESPW: East Sea Proper Water

Table 3.

Case	$r_{O2/P}$	$r_{P/P}$	$r_{N/P}$	$r_{Si/P}$	$r_{Corg/P}$	Ref.
1	-138	1	16	40	106	Redfield et al. (1963)
2	-170	1	15	40	117	Anderson and Sarmiento (1994)
3	-151	1	16	40	106	Anderson (1995)
4	-117	1	12.4	37	106	This study (2007)

Table 4.

CFCs – Min [1999]	
OUR (μmol·kg^{-1}·y^{-1})	Depth range (m)
2.9	200 – 600
1.0	600 – 1500
0.8	1500 – 2500
0.6	2500 – 3500
MBBM – Kim et al. [2003]	
2.0	200 – 1200
1.1	1200 – 2500
0.8	2500 - 3500

Table 5.

CASE 1			CASE 2			CASE 3			CASE 4		
$\Delta N^{deni}(\mu mol \cdot m^{-2} \cdot d^{-1})$			$\Delta N^{deni}(\mu mol \cdot m^{-2} \cdot d^{-1})$			$\Delta N^{deni}(\mu mol \cdot m^{-2} \cdot d^{-1})$			$\Delta N^{deni}(\mu mol \cdot m^{-2} \cdot d^{-1})$		
St.	MBBM	CFCs	St.	MBBM	CFCs	St.	MBBM	CFCs	St.	MBBM	CFCs
10	13.48	12.26	10	8.28	7.53	10	11.51	10.46	10	10.12	9.20
16	18.13	9.06	16	9.10	4.55	16	14.78	7.39	16	12.08	6.04
17	20.25	4.31	17	19.70	4.19	17	19.97	4.25	17	20.27	4.31
18	16.40	11.93	18	16.40	11.93	18	16.40	11.93	18	16.40	11.93
19	24.35	17.71	19	22.18	16.13	19	23.46	17.06	19	23.45	17.05
27	15.95	11.60	27	15.95	11.60	27	15.95	11.60	27	15.95	11.60
118	8.69	6.32	118	8.69	6.32	118	8.69	6.32	118	8.69	6.32
120	17.80	12.83	120	17.64	12.83	120	17.64	12.83	120	17.64	12.83
121	8.63	6.27	121	8.63	6.27	121	8.63	6.27	121	8.63	6.27
mean ± std	15.96±5.12	10.25±4.17	*mean ± std*	14.06±5.43	9.04±4.19	*mean ± std*	15.23±4.98	9.79±4.05	*mean ± std*	14.80±5.26	9.51±4.15

$$\overline{\Delta N^{deni}} \approx 9.0 - 16.0(\mu mol \cdot m^{-2} \cdot d^{-1}) = 6.38 - 11.35 \times 10^{4}(mol \cdot d^{-1})$$